Hindawi
Advances in Materials Science and Engineering
Volume 2021, Article ID 8855565, 15 pages
https://doi.org/10.1155/2021/8855565

Research Article

Investigation on the Influences of Curing Time on the Cracking Resistance of Semiflexible Pavement Mixture

Hua Tan,[1,2] **Zijia Xiong**,[3,4] **Minghui Gong**,[3,4] **Jie Chen**,[1,2] **and Jinxiang Hong**[3,4]

[1]*Guangxi Key Lab of Road Structure and Materials, No. 6,Gaoxin 2nd Road, Xixiangtang District, Nanning, China*
[2]*Guangxi Transportation Science and Technology Group, No. 6,Gaoxin 2nd Road,Xixiangtang District, Nanning, China*
[3]*Jiangsu Sobute New Materials Co.,Ltd., No. 118,Liquan Road, Nanjing, China*
[4]*State Key Laboratory of High-Performance Civil Engineering Materials, No. 118,Liquan Road, Nanjing, China*

Correspondence should be addressed to Hua Tan; 601503077@qq.com

Received 2 September 2020; Revised 22 January 2021; Accepted 28 January 2021; Published 27 February 2021

Academic Editor: Robert Černý

Semiflexible pavement (SFP) is constructed by pouring grouting material into porous asphalt (PA) mixture. SFP has been widely used to address the rutting distress issues across China in recent years. However, studies on its cracking resistance are limited and the failure mechanism of the SFP mixture has not been fully explored nor understood in a comprehensive way. Moreover, the influences of the curing time on the cracking property of the SFP mixture are still not clear. To this end, the strength development and shrinkage properties of grouting materials are determined by utilizing the three-point beam bending test and the shrinkage test. The semicircular bending (SCB) test and the scanning electron microscope-energy-dispersive spectrum (SEM-EDS) are conducted in this study to investigate the cracking resistance and failure mechanism of SFP mixtures with different curing days. Results show that both the strength and shrinkage of grouting materials would develop as the curing time was extended from 0 days to 14 days. SCB test results show that SFP mixtures have higher tensile strength but a lower flexibility index (FI) than PA mixture. It is found that the cracking resistance of SFP mixture is influenced by both the grouting materials' strength and shrinkage. SEM-EDS analysis demonstrates that the cement-asphalt interface is a stress concentration site and therefore is the weak zone where cracks would initially develop. The microcracks found in the interface zone with different curing days may contribute to the decline of the SFP mixture's anticracking ability. This study sheds light on the further application of SFP in practical projects.

1. Introduction

Semiflexible pavement is constructed by pouring cementitious slurry (fluidity <14 s) in porous asphalt pavement with air voids ranging from 20% to 30% [1–4]. After a certain curing time, the cementitious slurry hydrates and hardens. The flexible asphalt matrix and rigid cement both contribute to the excellent antirutting ability and high load bearing capacity while no joints are needed. In Europe and in Asia, this new type of pavement has been used as the pavement of highways, tunnels, and airport apron. With the aim of addressing the severe rutting distresses, SFP has been widely used in China in the past several years for intersections, bus stops, Bus Rapid Transit (BRT) lanes, and areas with frequent heavy-load vehicle starts and stops, which induce a high-level shearing force on the pavement [5–7]. It was found that the rutting depth of these aforementioned sections when using asphalt pavement would reach 5 cm after being in service for one summer. Annual maintenance is needed which is time- and labour-consuming. Since SFP is adopted to replace asphalt mixture as a top layer with a thickness around 6 cm, no rutting distress was observed [5]. However, transverse cracking (mostly reflective cracking) was found after the SFP was in service for 1-2 years. Thus, great attention has been drawn to the research of cracking resistance of such cement-asphalt composites [7]. More importantly, few researchers have made efforts to investigate the influences of curing time on the cracking resistance of

semiflexible pavement. This issue is critical because typically only a short curing time is allowed, especially in major cities. The high vehicle volume in such areas requires that the intersections repaired with SFP have to open to traffic as soon as possible to avoid serious traffic jams. Nevertheless, the mechanical properties as well as the cracking resistance of semiflexible pavement under different curing times are still unknown. Meanwhile, the relationship between curing time and cracking distress in SFP is not well established. To this end, this paper conducts a series of experiments to evaluate the properties of cement, asphalt matrix, and fabricated semiflexible pavement mixture with different curing days. Both macro- and micro-level researches are conducted to provide a fundamental insight into the cracking mechanism of semiflexible pavement.

In existing literature, Husain et al.'s research investigated the relationship between volumetric characteristics and properties of semiflexible pavement [8, 9]. Setyawan figured out the correlation between grouting materials' and SFP's compressive strength by considering the influences of aggregate, grouting materials, and asphalt [10]. It was shown in Koting et al.'s research that the SFP's mechanical properties (compressive strength, resilient modulus, and resistance to raveling performance) are closely related to the water/cement ratio of the grouting material. The replacement of 5% silica fume with an adequate amount of superplasticizer and water/cement ratio was beneficial in improving the properties of the cementitious grout [11, 12]. It was demonstrated in Hou et al.'s work that SFP performed better than conventional asphalt concrete mixture in high-temperature performance, fatigue resistance, and antimoisture susceptibility. The enhancement can be attributed to the bridge effect between cement paste and asphalt [13]. Zhang et al. pointed out that fluidity, strength, and drying shrinkage of cement paste vary with their compositions by comparing the performances of different grouting materials [14]. As found in Wang et al.'s work, the high-temperature rutting resistance, low-temperature cracking resistance, water damage resistance, and fatigue resistance of SFP were enhanced by adding Carboxyl Latex into cement mortar [15]. Mechanical properties and finite element analysis were both employed by Ding et al. to investigate the failure mechanism of SFP, which contains reclaimed asphalt pavement. The failure possibility order of each phase in recycled semiflexible pavement material was asphalt binder, reclaimed aggregate, cement paste, and virgin aggregate [16]. Yang and Weng revealed that the void content of porous asphalt mixture is the most important factor influencing the durability of SFP subjected to cyclic wheel load [17]. To sum up, lots of work has been done to promote the development of semiflexible pavement. Nevertheless, the influence of curing time on the cracking resistance of SFP is still unclear. Consoli et al. investigated the influence of curing time on the strength of cemented soil/sand and proved that strength increase of these materials has a close link with curing time [18–20]. As SFP is normally applied in the intersections which only allow a short construction window phase for not causing serious traffic jams, the curing period should be carefully controlled. With different curing periods, cementitious material within SFP will exhibit distinct strength characteristics and shrinkage property. It is notable that SFP is a complex composite which contains aggregate phase, asphalt binder phase, cement network phase, interface between aggregate and asphalt binder, and interface between asphalt binder and cement. Shrinkage of cementitious material may cause stress concentration in the interface area which would become the origin of cracks and deteriorate the pavement performance of composite [21]. Nevertheless, limited research has been done addressing the failure mechanism of asphalt binder-cement interface during shrinkage with different curing times. In this regard, more work needs to be done to fill in the gap to provide guidance for determining appropriate curing period and for selecting suitable cementitious grouting material for SFP.

In this paper, the flexural strength and compressive strength of grouting materials were measured as curing time changed from 3 days to 14 days. The shrinkage property of grouting materials was measured at different curing times. Semiflexible pavement mixtures were fabricated and cured together with grouting materials. Samples with different curing times were tested by utilizing the Semicircular Bending test to evaluate their tensile strength, fracture energy, and flexibility index. The relationship between the properties of grouting materials and the cracking resistance of semiflexible mixture was then investigated. Scanning Electron Microscope and Energy-Dispersive Spectrum was employed to provide an insight into the cement-asphalt interface strength formation mechanism. The research methodology of this study is presented in Figure 1.

2. Materials and Methods

2.1. Materials

2.1.1. Grouting Materials. The grouting materials (commercial product of Jiangsu Sobute New Materials Co., Ltd.) used in this paper were composed of silicate cement, fine aggregate, and various admixtures. The cement is the type of 42.5 MPa. The admixtures contained agent of early strength and retarder. The cement content of the grouting materials was around 60 wt%. Slurry was prepared by using a high shear mixer (5000 rmp ∗2 minutes) with a water-to-grouting material ratio (by weight) of 0.3. The fluidity of slurry was approximately 14 seconds as measured through the Leeds Flow Cone test. The slurry was cast into the mould to prepare the prismatic beams with a size of $40 \times 40 \times 100$ mm. These beams were further tested to acquire the flexural strength, compressive strength, and shrinkage property of grouting materials.

The asphalt, cement, and the filler are the common materials. Asphalt is consisted by some organic material. Filler is a type of limestone powder. And the cement mainly contains the elements of O, Si, C, and Al. There are significant differences of these materials.

2.1.2. Mixture. A gradation of semiflexible asphalt concrete-13 (SFAC-13) was selected to prepare the SFP mixture samples, which is shown in Table 1. The aggregate is basalt

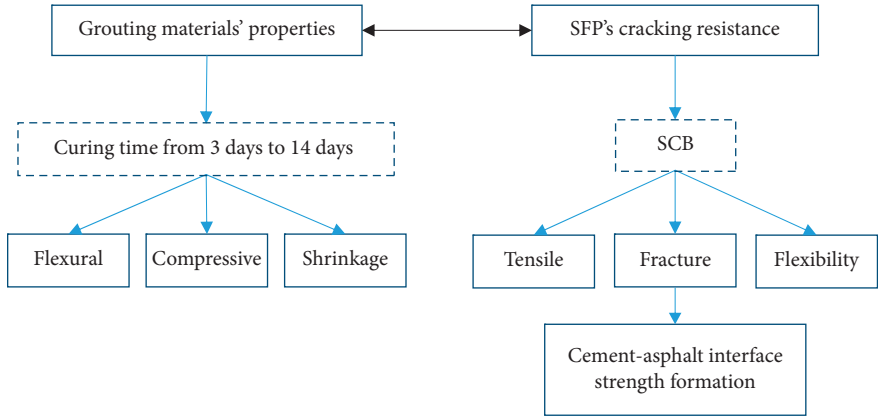

Figure 1: Research methodology.

Table 1: Gradation of SFAC-13.

Sieve size, mm	16	13.2	4.75	2.36	0.6	0.3	0.15	0.075
Passing percentage, %	100	93.4	19.5	12.5	8.2	5.4	4.9	2.5

coarse, and filler is limestone mineral powder. SBS-modified asphalt, MA additive (one polymer modifier developed by Sobute New Materials Co. Ltd.), lignin fiber, basalt coarse aggregate, and limestone mineral powder were used as raw materials. MA additive is a modifier of asphalt. It contrasted by rubber, plastic, and solubilizer. It is mixed with asphalt to enhance the flexibility and adhesion. Properties of the SBS-modified asphalt and coarse aggregate are listed in Tables 2 and 3, respectively. MA additive (14 wt% of SBS-modified asphalt binder) and lignin fiber (0.2 wt% of asphalt mixture) were incorporated in asphalt mixture by using the dry mixing method [7]. Cantabro and drainage tests were used to determine the optimum asphalt content, which was found to be 4.2%. The tested properties of PA mixture are shown in Table 4.

Porous asphalt (PA) mixture used for grouting was compacted to air voids of 26 ± 1% by using 50 gyrations with the Superpave Gyratory Compactor (SGC). The aggregate was heated to 185°C and the asphalt binder was heated to 160°C. The compaction temperature was set at 180°C. Each PA sample was 150 mm in diameter and 140 mm in height. After the PA samples were cooled to room temperature, their bottom-face and side-face were sealed with tapes. The slurry was then poured into the PA samples from the top side. All of the SFP samples were cured in a room with a temperature of 25°C and a humidity of 90%. The different curing periods were selected as 3, 4, 5, 7, and 14 days.

2.2. Test Methods

2.2.1. Three-Point Bending (TPB) Test. At different specific curing times, the prismatic beam (40 mm∗40 mm∗160 mm) was tested by the three-point bending test. The flexural strength of prismatic beams can be calculated as follows [22]:

$$\sigma_f = \frac{3F_{fu}l}{2bh^2}, \quad (1)$$

where F_{fu} = ultimate load (N); l = length (mm); and b = thickness (mm) and h = height (mm).

2.2.2. Compression Test. Prismatic cubes from the fractured TPB beams were further tested in the compression test with the universal testing machine, as shown in Figure 2. Compressive strength was calculated as F_{fu}/S [22], where S = area of the cross section.

2.2.3. Shrinkage Test. The 40 × 40 × 100 mm prismatic beam was used to measure the drying shrinkage of grouting materials. Three replicates were tested for each test. After demolding, all of the prisms' initial length comparator reading was recorded after 24 h. The prisms were then cured in a chamber for different days at a temperature of 20°C with a relative humidity of 90% for subsequent measurements. A length comparator was used to measure the dimensional changes in beam samples. Length measurements were conducted at 3, 5, 7, and 14 days, respectively. Shrinkage was calculated by dividing the change in dimensions by the initial length of the prismatic specimen [23]. The samples and test setup are shown in Figure 3.

2.2.4. Semicircular Bending (SCB) Test. Half-moon-shaped specimens cut from SGC compacted asphalt mixture were utilized for the SCB test with UTM-30. Four replicates were tested for each test. The height, thickness, and diameter of the SCB specimen were 50 mm, 50 mm, and 150 mm, respectively. The target notch depth and width were 15 mm and 1.5 mm. The test was conducted by applying monotonic loading on the specimens supported by two bars. The samples and test setup of SCB test are shown in Figure 4.

The tensile strength, fracture energy, and flexibility index (FI) were calculated. Tensile strength can be calculated as [24, 25]

Table 2: Property of SBS-modified asphalt.

Penetration (100 g, 25°C), 0.1 mm	Softening point, °C	Ductility (5°C), cm	Viscosity (135°C), Pa·s
54	62	30	2.0
	RTFOT		
Penetration ratio (100 g, 25°C), 0.1 mm	Ductility (5°C), cm	Quality change (%)	
67	31	−0.05	

Table 3: Property of aggregate.

Properties	Aggregate
Apparent specific gravity	2.85
Bulk specific gravity	2.81
Absorption, %	0.6

$$S = \frac{4.976F}{B\ D}, \tag{2}$$

S is tensile strength, MPa; F is the value of peak load, N; B is the thickness of the specimen, mm; and D is the ligament of the specimen, mm.

Fracture energy (G_f) can be expressed as

$$G_f = \frac{W_f}{B\ D} \times 10^6, \tag{3}$$

G_f is fracture energy, J/m^2; W_f is the work of fracture, J.

FI at 25°C can be calculated as

$$FI = \frac{G_f}{|m|} \times 0.01, \tag{4}$$

$|m|$ is the absolute value of postpeak loading slope m, kN/mm.

2.2.5. Scanning Electron Microscope-Energy-Dispersive Spectrum (SEM-EDS). In this study, the cement-asphalt interfacial microstructure of the SFP was observed by using a Scanning Electron Microscope (SEM), QUANTA 250. This device was equipped with a cold field-emission electron gun operating at 15 kv. The SCB sample was cut into small pieces and then dried in a vacuum drying oven until the constant weight was reached. Finally, the surface of the sample was sputter-coated with a thin layer of Pt before SEM observation and EDS analysis. The samples and test setup of SEM-EDS test are shown in Figure 5.

3. Results and Discussion

3.1. Flexural and Compression Test. The flexural strength and compressive strength of grouting materials at different curing days are displayed in Figure 6. It can be seen that the strength of grouting material increases sharply after 3 days' curing process. However, only a slight increase in grouting materials' strength can be seen with further curing. It is also notable that there are fluctuations in the curves of both flexural and compressive strength data. Decreases in the grouting material's strength are found after 5 days' curing, and then a constant increase can be seen in both the flexural and compressive strength curves as curing days extend.

To further check the validity of the grouting material's strength data, Pearson's correlation analysis was conducted to investigate the correlation between curing days and strength. The relevant results are shown in Table 5. The data is divided into two groups for analysis. Group 1 contains strength data with a curing period of 0 to 14 days while the second group only contains strength data after a curing period of 3 days. It is shown in Table 5 that there is a strong correlation between curing days and the strength of grouting materials. However, for the data with the curing days of 3 to 14 days, the Pearson correlation coefficient falls to 0.58, which reveals that there is only a moderate correlation between the curing period and compressive strength. On the other hand, Pearson's correlation analysis results indicate that there is a very strong correlation between curing days and the flexural strength of grouting materials with a Pearson correlation coefficient of 0.82. Based on the Pearson correlation analysis results, it is generally found that curing time has a more profound influence on the growth of flexural strength than compressive strength. The Pearson correlation coefficient results of group 2 shows that the flexural strength of grouting materials still goes up after 3 days' curing, while extending the curing time does not contribute to the increase of grouting materials' compressive strength after 3 days' curing period.

3.2. Shrinkage Test. The shrinkage of the grouting material's prismatic beam with different curing days is measured and displayed in Figure 7. It is apparent that the shrinkage of grouting material keeps increasing as the curing time extends. The 1st derivative of the shrinkage coefficient-curing period curve is also determined and shown in Figure 8. As it can be seen, the increasing rate of shrinkage is relatively high in the first 3 days which indicates that the shrinkage of grouting materials develops quickly in the beginning.

3.3. Semicircular Bending Test. The force-displacement curves of the SFP and PA samples are shown in Figure 9. It can be seen from Figure 9(a) that all the curves reach their peaks at a displacement of around 2 mm. The peak forces of four replicates range from 2.75 to 3.5 kN, and all the curves end before the displacement of 12 mm. For Figure 9(b), the curves of the SFP samples and PA sample are displayed together for comparison. It is obvious that the SFP's curve is steeper than the PA's which may correspond to the brittleness of SFP. Generally, the SFP samples cured for 7 and 14 days have higher peak force values than other samples. It is interesting to see that the SFP sample cured for 4 days exhibits distinct postpeak behavior. The postpeak force from that curve declines more slowly than the curves of the other SFP mixtures, which corresponds to more ductility when

Table 4: Properties of PA mixture.

Properties	Bitumen aggregate ratio (%)	Total void ratio (%)	Connected void ratio (%)	Marshall's stability (kN)	Flow value (0.1 cm)	Leakage loss (%)	Cantabro loss (%)
Index value	4.2	25.9	24.1	3.4	22.6	0.12	28

Figure 2: TPB test and compression test setup.

Figure 3: Samples and test setup of shrinkage test.

Figure 4: Samples and test setup of SCB test.

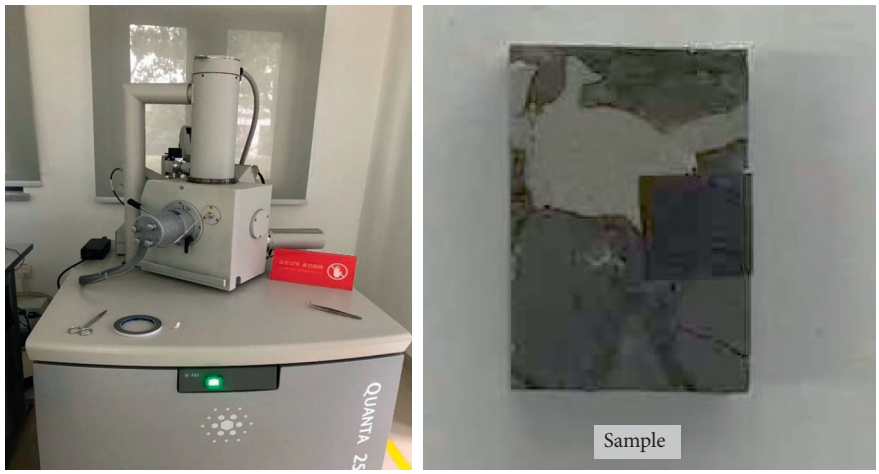

Figure 5: Samples and test setup of SEM-EDS test.

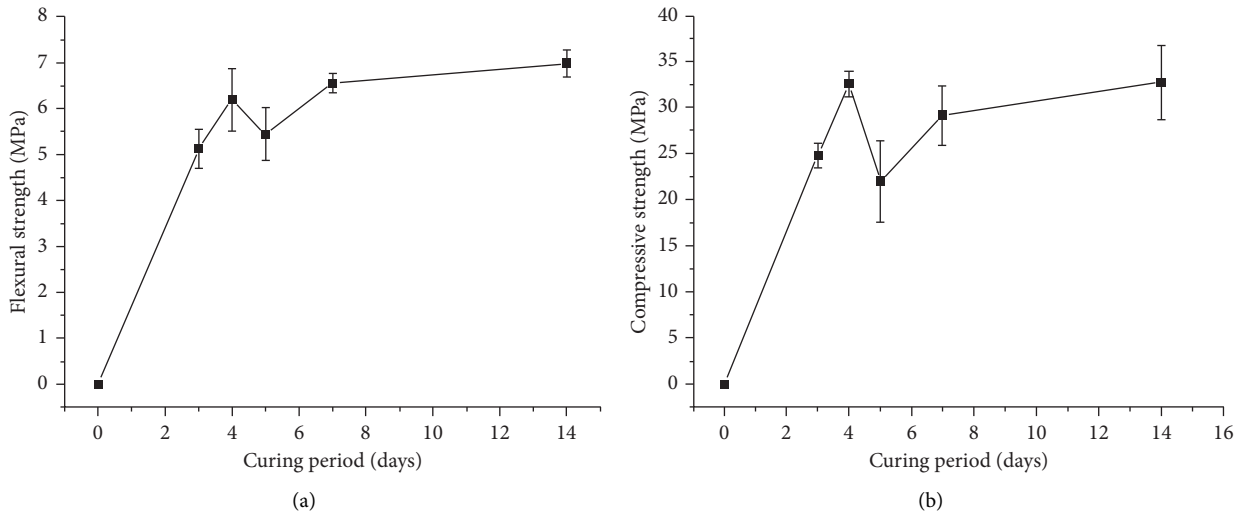

Figure 6: Flexural and compressive strength of grouting materials with different curing times. (a) Flexural strength. (b) Compressive strength.

Table 5: Pearson's correlation analysis results of grouting materials' strength data.

Data group	Pearson's correlation coefficient	
	Flexural strength (MPa)	Compressive strength (MPa)
Group 1 (0–14 curing days)	0.72	0.68
Group 2 (3–14 curing days)	0.82	0.54
Appendix		
Very strong correlation	>0.8, <−0.8	
Strong correlation	0.6~0.8, −0.6~−0.8	
Moderate correlation	0.4–0.6, −0.4~−0.6	
Weak correlation	0.2–0.4, −0.2~−0.4	
Very weak correlation	<0.2, >−0.2	

cracking extends. Unlike the SFP mixture, the PA mixture's force-displacement curve exhibits a much lower peak force value and its postpeak curve is not as steep as that of the SFP mixture. This may indicate that cracks in PA occur more easily but develop much slower when compared with SFP mixture. As shown in Figure 9(c), the failure displacement for grouting material is much smaller than that of porous asphalt mixture and SFP. Moreover, the force drops much faster than other two kinds of mixtures, which shows no ductile characteristics.

The tensile strength of all the samples is extracted from their force-displacement curves and is shown in Figure 10.

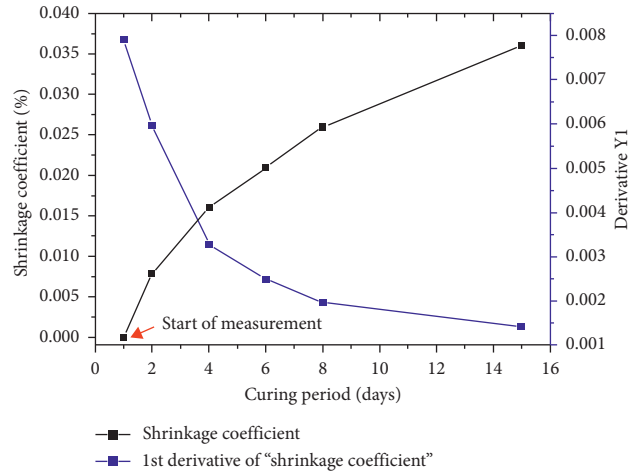

Figure 7: Shrinkage with different curing times.

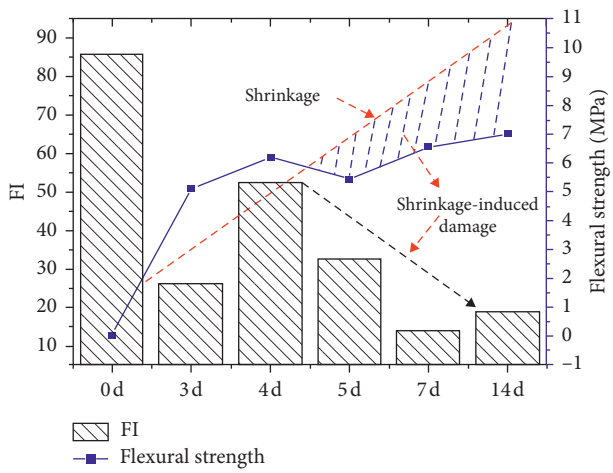

Figure 8: FI of SFP specimen and flexural strength of grouting material with different curing days.

The PA sample has the lowest tensile strength, which is almost half of that of the SFP mixtures. For the SFP mixtures, the tensile strength increases as the curing period extends from 3 days to 14 days except for the data in the 5th day. The low tensile strength of the PA mixture may result from its high air void content. In the SFP mixture, the grouting materials fill in the gaps within the asphalt mixture skeleton and the strong bond between the grouting materials and the asphalt positively contributes to the high tensile strength. However, Figure 11 shows that the SFP mixture's fracture energy rises first as curing begins and reaches its highest level in the 4th day. After that, the fracture energy begins to decrease as curing goes on. It is interesting to find that PA mixture and SFP mixture cured for 7 and 14 days have similar fracture energy results. From this point, the increase of grouting materials' strength does not contribute to the growth of the SFP mixture's fracture energy. This can be verified in Table 6 that grouting materials with different curing days exhibit similar fracture energies, which are much lower than PA and SFP. More interestingly, Figure 12 shows that the PA mixture has a much higher flexibility index (FI) value than the SFP mixtures. As the grouting material begins to harden, the FI value of SFP decreases from 85 for the sample cured for 0 days (PA mixture, namely) to 26 for the sample cured for 3 days. The SFP mixture's FI value then goes up and reaches 53 at the 4th day. After that, the FI value of SFP decreases as the curing period extends. Ultimately, the FI value of the SFP mixture cured for 14 days is measured as 19. For SFP mixtures with curing days from 3 days to 14 days, it seems that both the FI and fracture energy results demonstrate similar trends, indicating that the SFP mixture cured for 4 days has the best anticracking ability. Moreover, it can be seen from Figures 11 and 12 that the PA mixture and SFP mixture cured for 7 and 14 days have similar fracture energies but different FI values. This may be related to the different postpeak behaviors which are shown in Figure 9(b). The m value of the PA mixture in equation (3) is much lower than that of the SFP mixtures, which makes the PA mixture's FI value much higher.

3.4. Relationship between the Grouting Material's Strength and the SFP Mixture's Anticracking Property. The tensile strength and FI of SFP mixtures and the flexural strength of grouting materials with different curing days are cross-compared in Figures 8 and 13, respectively. It is clearly shown in Figure 13 that both SFP specimens' tensile strength and grouting materials' flexural strength show similar trends with different curing days. All the SFP mixtures have the same asphalt mixture skeleton but different grouting materials with different mechanical properties. The results in Figure 13 indicate that the development of the SFP mixture's tensile strength is highly contributed to the increase of the grouting materials' flexural strength. This can be possibly explained as that both the SFP sample and the grouting material sample are bent in either the SCB test or the TPB test, in which they are fractured under tension.

As it can be seen in Figure 8, even though grouting material cured by 0 days provides no strength in SFP mixture, the sample still has a high FI value. As the flexural strength of grouting material increases from the 3rd day to the 4th day, the anticracking ability of the SFP mixture, as

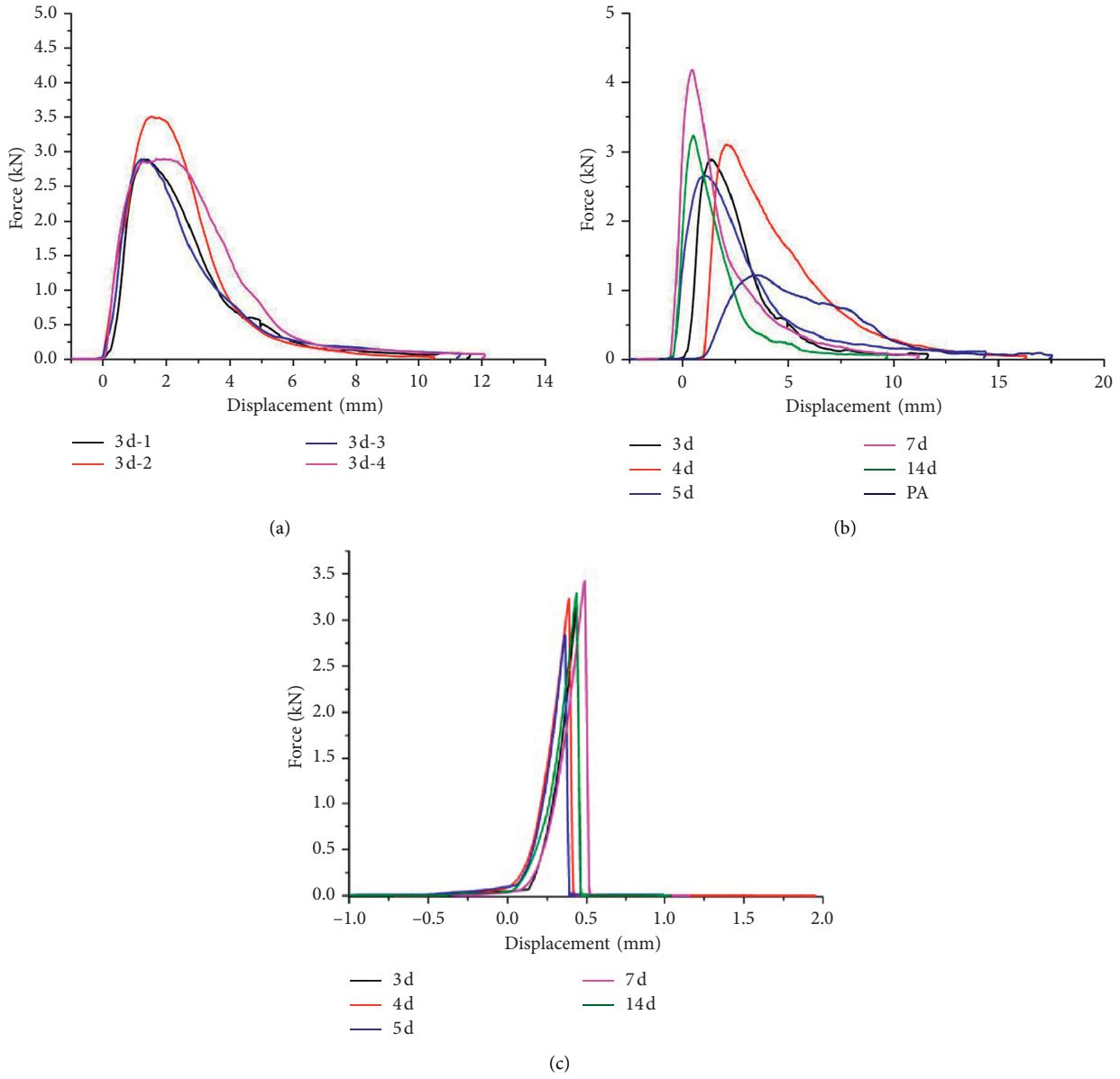

Figure 9: Force-displacement of SFP sample and PA sample. (a) 3 days' cured SFP samples. (b) SFP samples and PA sample. (c) Grouting materials with different curing days.

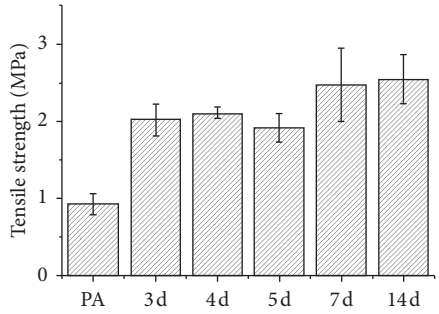

Figure 10: Tensile strength of PA and SFP specimen with different curing days.

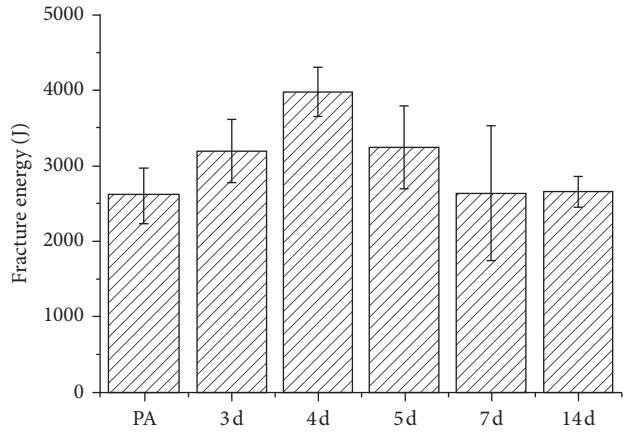

Figure 11: Fracture energy of PA and SFP specimen with different curing days.

Table 6: Fracture energy of grouting materials with different curing days.

Curing days, d	3	4	5	7	14
Fracture energy, J	129	151	145	154	153
Std. deviation	0.2723	0.0281	0.2247	0.0918	0.0215

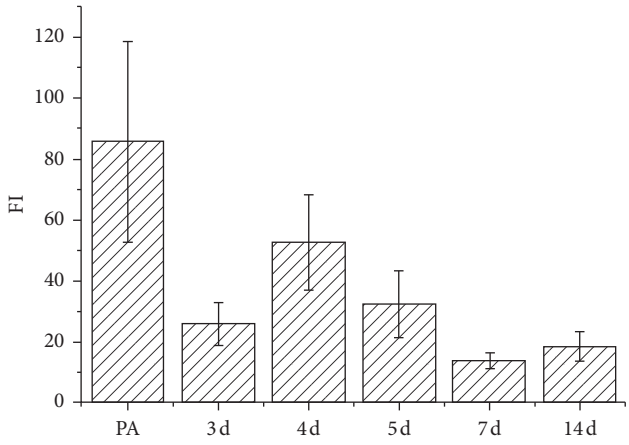

Figure 12: FI of PA and SFP specimen with different curing days.

measured by the FI value, is also enhanced. However, the decrease of the SFP mixture's FI value is found as the flexural strength of the grouting material goes up from the 5th day to the 14th day. Nevertheless, the red schematic curve in Figure 8 may indicate that the drop of SFP mixture's FI can be attributed to the shrinkage of grouting material. This result may prove that there is a competition between the grouting materials' strength increase and the shrinkage increase regarding the SFP mixture's anticracking ability. The hydration of grouting materials would contribute to both the formation of a rigid network filling in asphalt mixture skeleton and an interface strength increase between asphalt and cement. The rigid cement network and interface would contribute to the increase of SFP mixture's tensile strength. However, the development of this shrinkage may induce microcracks in the SFP mixture. As the cracking happens in the beginning, the hydration product may be able to fill up the tiny cracks and make SFP mixture's FI value increase further. However, as the hydration rate of grouting materials slows down and the shrinkage continues developing, the cracks can no longer be filled up and these cracks may interconnect, which results in the decrease of the SFP mixture's FI value.

3.5. SEM-EDS. SEM was used to observe the morphology of SFP mixture cured for different amounts of days. In order to identify the asphalt binder, cement and aggregate in SEM, EDS was used to analyze the element components of different phases. As shown in Figure 14, three spots are selected to conduct the test. Element analysis results are displayed in Figure 15. It is illustrated in Figure 15(a) that the materials in Spot 1 mainly consist of O, Si, and Ca which may come from the mineral filler. The spot 2 EDS result indicates that the

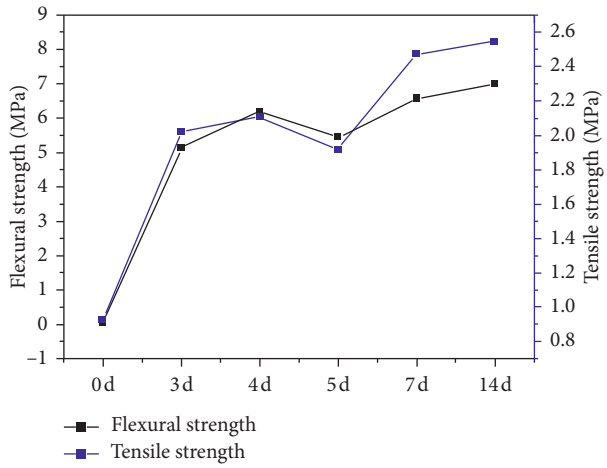

Figure 13: Tensile strength of SFP specimen and flexural strength of grouting material with different curing days.

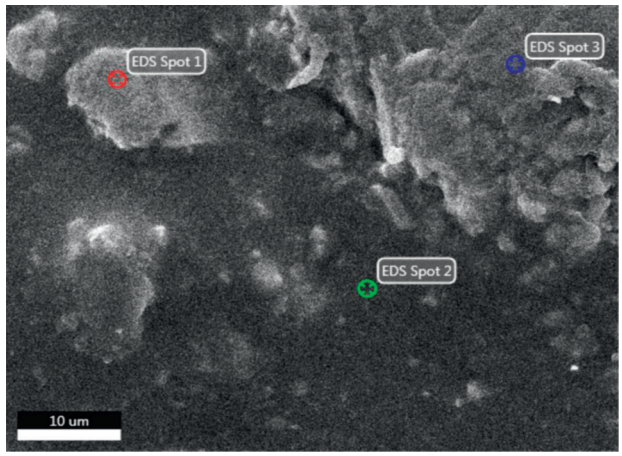

Figure 14: Schematic of EDS spots.

dark phase in Figure 14 can be attributed to the asphalt binder since its carbon element weight is higher than 80%. Based on results from Figure 15(c), it is believed that the materials in the right-top of Figure 14 are grouting materials. It mainly contains the elements of O, Si, C, and Al.

Element sweep analysis is further conducted across the interface which is marked with a yellow line in Figure 16. The results clearly show that the darker phase is a carbon-based material while the material from right-down in the morphology image is the grouting materials which mainly consist of Si, Al, and O.

Images of interfaces from SFP mixtures cured for different amounts of days are shown in Figures 17–21. It is found from Figure 17 that there are some pores in the cement/aggregate-asphalt interface that indicate that the grouting material/aggregate and asphalt binder may not be fully bonded in the SFP mixture. It is interesting to see that there are some cracks along the interface after 4 days' curing. The appearance of cracks may be attributed to the shrinkage of cement materials or the materials failure during the SCB test. It is also notable that there are several cracks in the asphalt binder phase which are 30 to 40 micrometers away from the cement-asphalt interface. It seems that the interface bond is strong while the crack failures mainly take place in the asphalt binder and cement near the interface area. For samples cured for 5 days, the loose cement structure induced by cracks is found. It is shown from the SCB results that the anticracking ability of SFP begins to fall after 4 days' curing. The microscopy results herein indicate that the deterioration of the SFP mixture's performance may result from the development of cracks in the grouting materials along the cement-asphalt interface.

When comes to the sample cured for 7 and 14 days, it is obvious that the asphalt binder surface is much flatter than that of the grouting material. The uneven morphology can be attributed to the pores and defects in cementitious materials and maybe the microdamage induced by the polishing and grinding process during sample preparation. Moreover, the

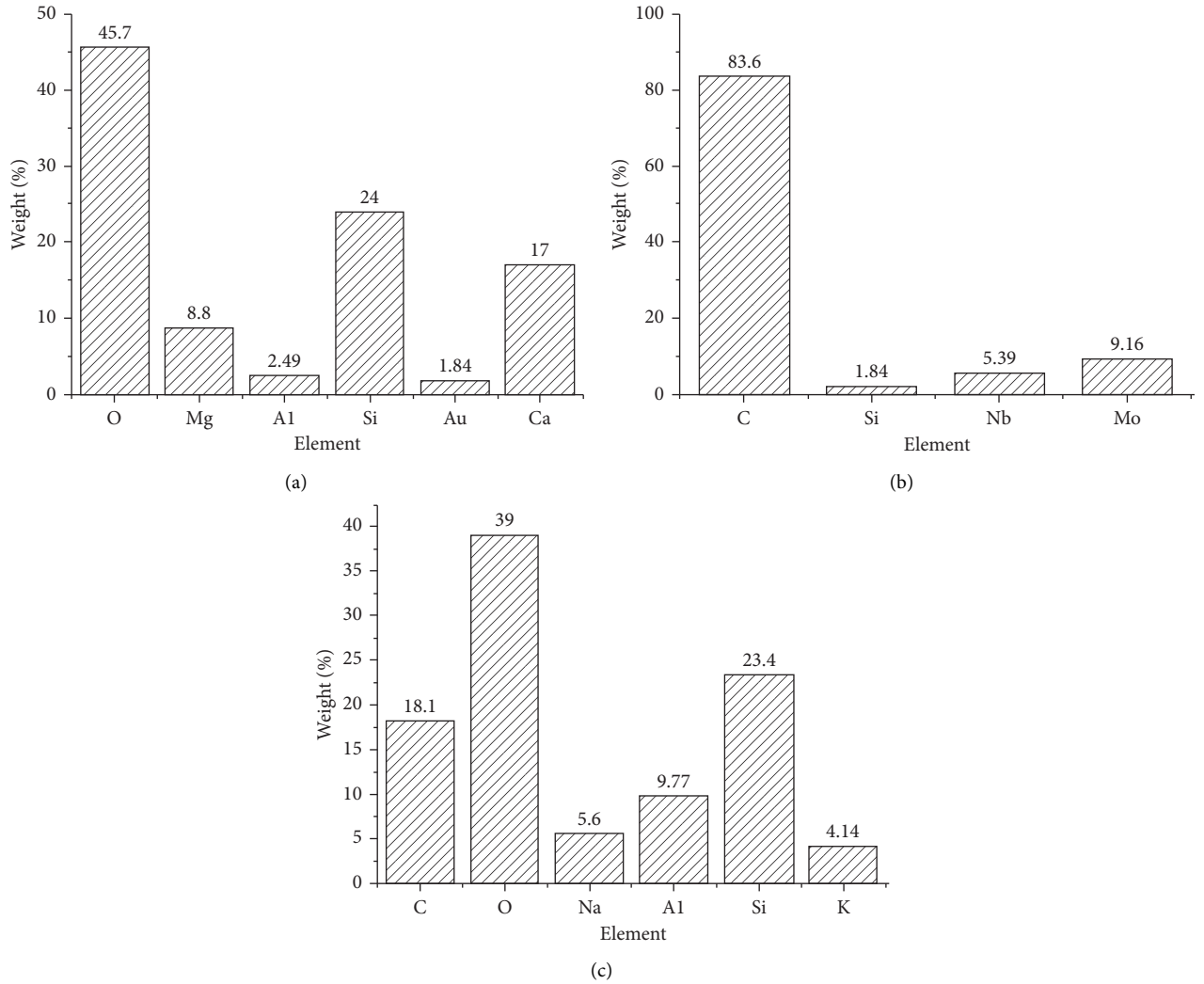

Figure 15: EDS results of SFP mixture. (a) Spot 1. (b) Spot 2. (c) Spot 3.

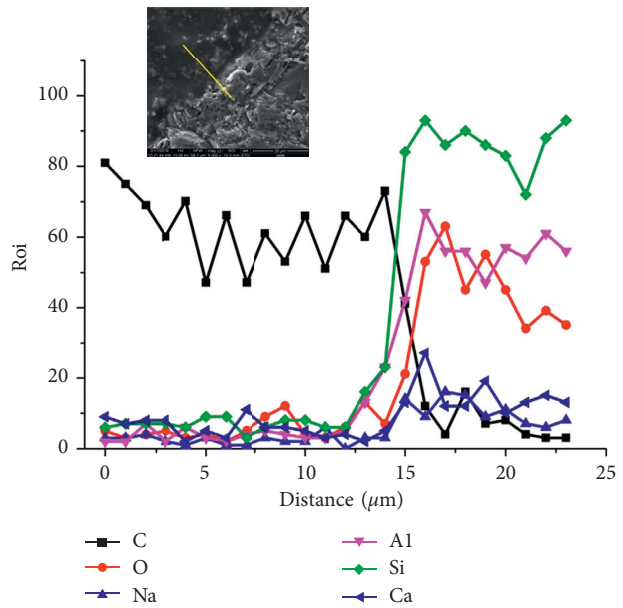

Figure 16: Element sweep analysis result of the SFP interface.

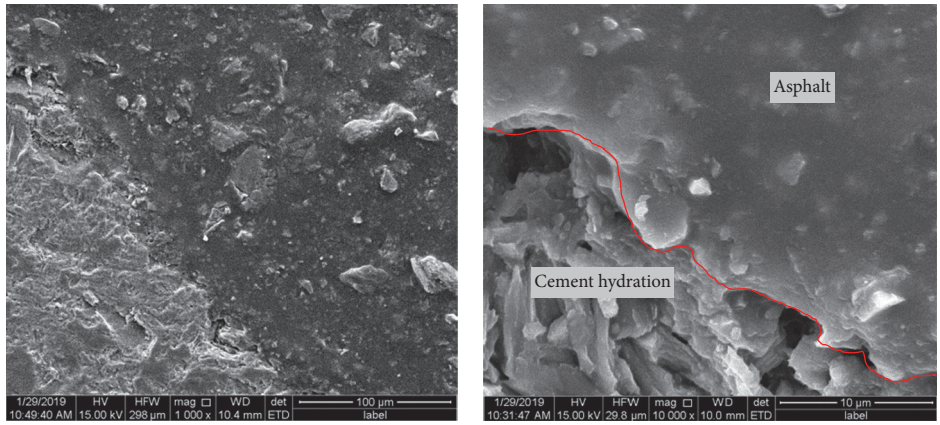

(a) (b)

Figure 17: Morphology of SFP sample cured by 3 days. (a) Scale bar = 100 μm. (b) Scale bar = 10 μm.

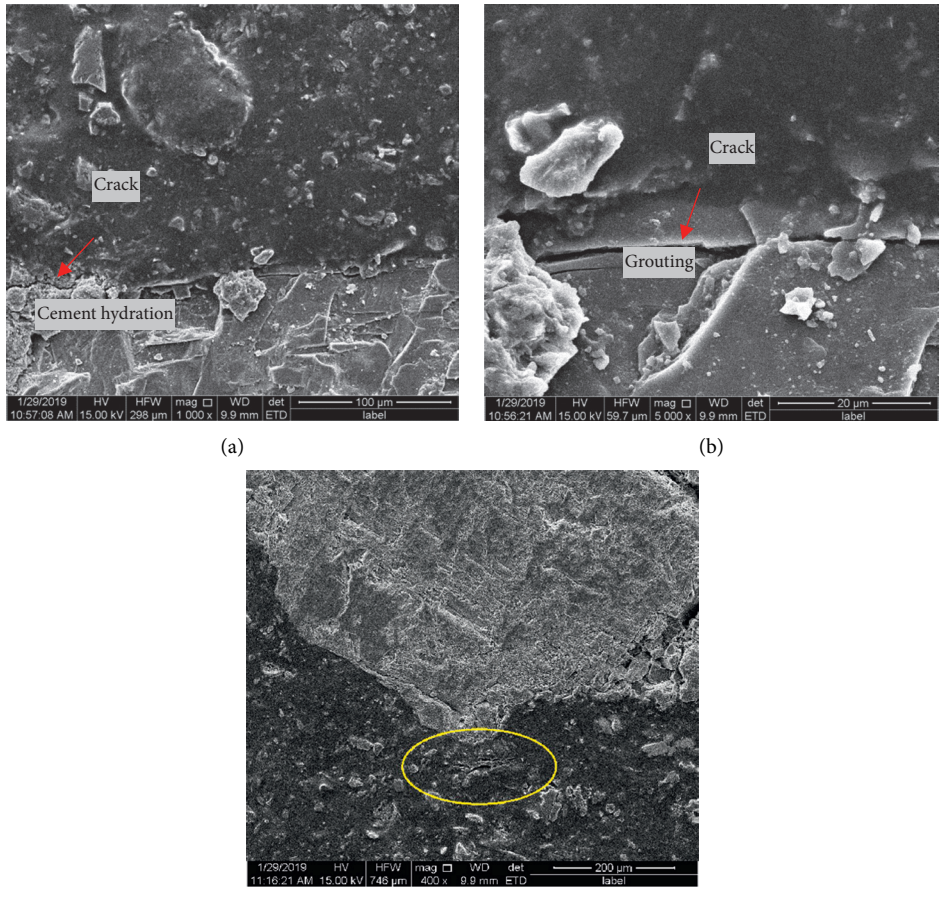

(a) (b)

(c)

Figure 18: Morphology of SFP sample cured for 4 days. (a) Scale bar = 100 μm. (b) Scale bar = 20 μm. (c) Scale bar = 200 μm.

asphalt phase seems to detach from the grouting materials which can be regarded as adhesive failure. A few microcracks are detected on the surface of the sample cured for 14 days. However, the observed microcracks are much shorter and narrower than those found in Figure 20. This result shows that the deterioration of the SFP mixture's property during curing mainly comes from the failure near the interface rather than in the bulk rigid cement.

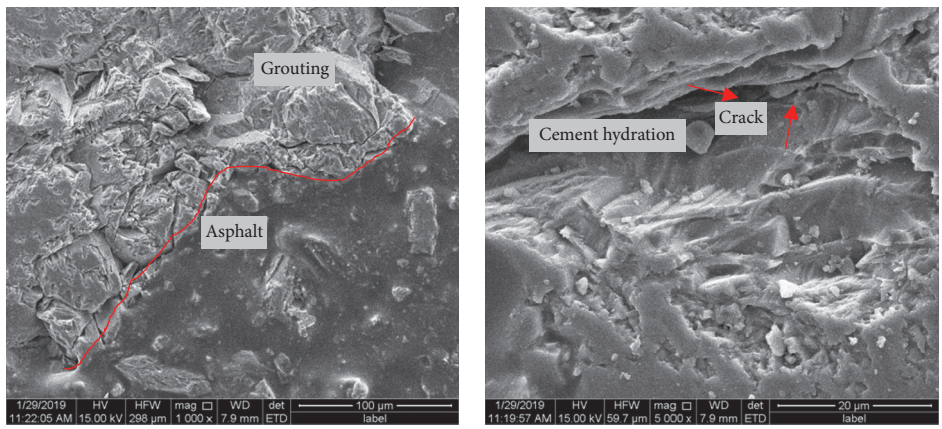

(a) (b)

Figure 19: Morphology of SFP sample cured for 5 days. (a) Scale bar = 100 μm. (b) Scale bar = 20 μm.

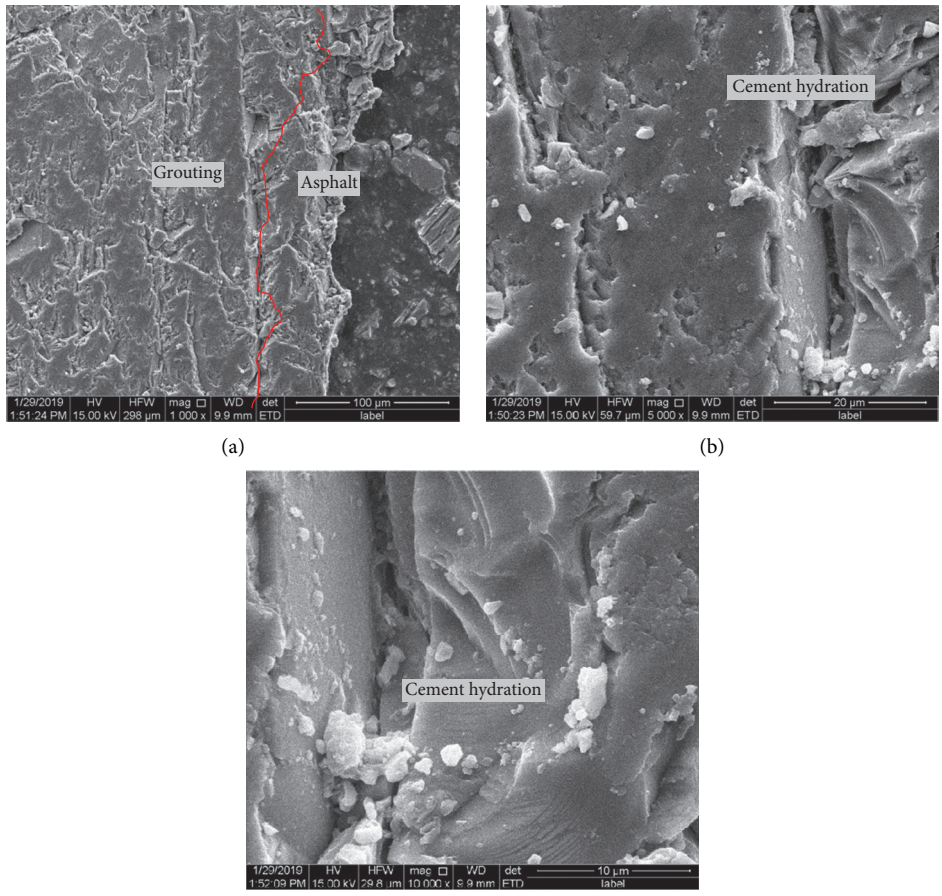

(a) (b)

(c)

Figure 20: Morphology of SFP sample cured for 7 days. (a) Scale bar = 100 μm. (b) Scale bar = 20 μm. (c) Scale bar = 10 μm.

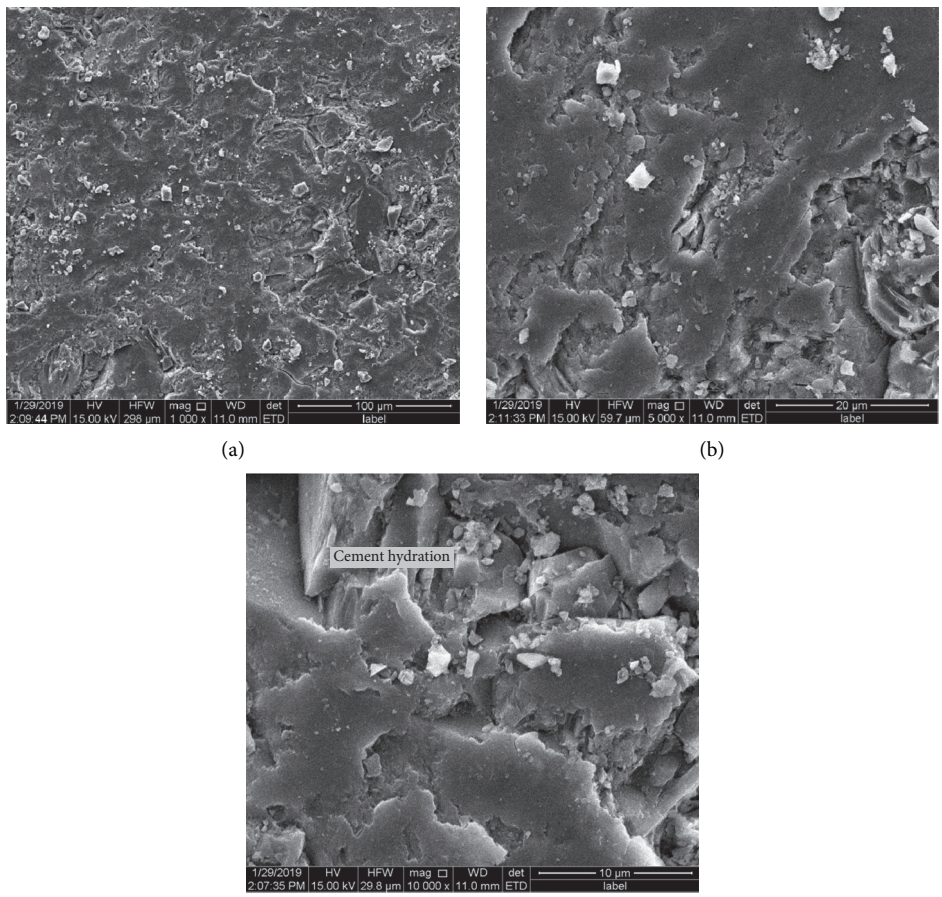

Figure 21: Morphology of SFP sample cured for 14 days. (a) Scale bar = 100 μm. (b) Scale bar = 20 μm. (c) Scale bar = 10 μm.

4. Conclusions

The mechanical properties of grouting materials and SFP mixtures with different curing days are characterized by using the three-point beam bending test and the semicircular bending test, respectively. The shrinkage property of grouting materials is also studied. The morphology of the SFP interface at microscale is also investigated with SEM-EDS. Conclusions are drawn as follows:

(1) Both the strength and shrinkage of grouting materials would develop as the curing time extended from 0 days to 14 days. It is shown that the grouting material's compressive strength is much higher than its flexural strength.

(2) The SCB test results show that SFP mixtures have a higher tensile strength than PA mixture. However, the PA mixture and the SFP mixture cured for 7 and 14 days exhibit similar fracture energies. It is interesting to find that the fracture energy of SFP mixture reaches its highest value after 4 days' curing and it begins to decline as curing time extends. FI results show that the PA mixture has much better anticracking ability than the SFP mixtures.

(3) A strong relationship can be found between grouting materials' flexural strength and SFP mixture's tensile strength. The evolution of the SFP mixture's anticracking ability with different curing days can be divided into two stages. The first stage is mainly influenced by the development of the grouting materials' flexural strength while the second stage seems to be mainly affected by the shrinkage of the grouting materials.

(4) SEM-EDS analysis was conducted on the SFP sample surface and the result shows that cracks tend to initiate mainly in the cement near the cement-asphalt interface. This could be explained as that the grouting materials are a stress-tolerant material while the asphalt binder is a strain-tolerant material. The interface between these two materials is a stress concentration site and the grouting materials would first reach their failure limit due to shrinkage and external load.

Data Availability

The data used to support the findings of this study are available from the corresponding author upon request.

Conflicts of Interest

The authors declare that they have no conflicts of interest regarding the publication of this paper.

Acknowledgments

The authors gratefully acknowledge the financial support of the Open Fund of Guangxi Key Laboratory of Road Structure and Materials (2020gxjgclkf006).

References

[1] I. L. Al-Qadi, H. Gouru, and R. E. Weyers, "Asphalt portland cement concrete composite: laboratory evaluation," *Journal of Transportation Engineering*, vol. 120, no. 1, pp. 94–108, 1994.

[2] J. Pei, J. Cai, D. Zou et al., "Design and performance validation of high-performance cement paste as a grouting material for semi-flexible pavement," *Construction and Building Materials*, vol. 126, pp. 206–217, 2016.

[3] M. L. Afonso, M. Dinis-Almeida, L. A. Pereira-de-Oliveira, J. Castro-Gomes, and S. E. Zoorob, "Development of a semi-flexible heavy duty pavement surfacing incorporating recycled and waste aggregates-preliminary study," *Construction and Building Materials*, vol. 102, pp. 155–161, 2016.

[4] J. Cai, J. Pei, Q. Luo, J. Zhang, R. Li, and X. Chen, "Comprehensive service properties evaluation of composite grouting materials with high-performance cement paste for semi-flexible pavement," *Construction and Building Materials*, vol. 153, pp. 544–556, 2017.

[5] C. Deng, C. Huang, J. Hong, T. Zhao, and D. Zhang, "The study of super-early-strength semi-flexible pavement used in municipal road," *Highway Engineering*, vol. 41, no. 1, pp. 116–119, 2016.

[6] Y. Du, J. Chen, Z. Han, and W. Liu, "A review on solutions for improving rutting resistance of asphalt pavement and test methods," *Construction and Building Materials*, vol. 168, pp. 893–905, 2018.

[7] M. Gong, Z. Xiong, H. Chen et al., "Evaluation of the cracking resistance of semi-flexible pavement mixture by laboratory research and field validation," *Construction and Building Materials*, vol. 207, pp. 387–395, 2019.

[8] Q. J. Ding, Z. Sun, F. Shen, and S. L. Huang, "The performance analysis of semi-flexible pavement by the volume parameter of matrix asphalt mixture," *Advanced Materials Research*, vol. 168–170, pp. 351–356, 2011.

[9] N. M. Husain, M. R. Karim, H. B. Mahmud, and S. Koting, "Effects of aggregate gradation on the physical properties of semiflexible pavement," *Advances in Materials Science and Engineering*, vol. 2014, Article ID 529305, 8 pages, 2014.

[10] A. Setyawan, "Asessing the compressive strength properties of semi-flexible pavements," *Procedia Engineering*, vol. 54, pp. 863–874, 2013.

[11] S. Koting, M. Rehan, and H. Mahmud, "The properties of bituminous mixtures for semi-flexible pavement," in *Proceedings of the 7th International Conference of Eastern Asia Society for Transportation Studies*, vol. 6, Dalian, China, September 2007.

[12] S. Koting, M. Karim, H. Mahmud et al., "Effects of using silica fume and polycarboxylate-type superplasticizer on physical properties of cementitious grout mixtures for semiflexible pavement surfacing," *The Scientific World Journal*, vol. 2014, Article ID 596364, 7 pages, 2014.

[13] S. Hou, T. Xu, and K. Huang, "Investigation into engineering properties and strength mechanism of grouted macadam composite materials," *International Journal of Pavement Engineering*, vol. 17, pp. 1–9, 2016.

[14] J. Zhang, L. Cai, L. Pei, R. Li, and X. Chen, "Formulation and performance comparison of grouting materials for semi-flexible pavement," *Construction and Building Materials*, vol. 115, pp. 582–592, 2016.

[15] D. Wang, X. Liang, C. Jiang, and Y. Pan, "Impact analysis of carboxyl latex on the performance of semi-flexible pavement using warm-mix technology," *Construction and Building Materials*, vol. 179, pp. 566–575, 2018.

[16] Q. Ding, M. Zhao, F. Shen, and X. Zhang, "Mechanical behavior and failure mechanism of recycled semi-flexible pavement material," *Journal of Wuhan University of Technology (Materials Science Edition)*, vol. 30, no. 5, pp. 981–988, 2015.

[17] B. Yang and X. Weng, "The influence on the durability of semi-flexible airport pavement materials to cyclic wheel load test," *Construction and Building Materials*, vol. 98, pp. 171–175, 2015.

[18] N. Consoli, R. Cruz, and M. Floss, "Variables controlling strength of artificially cemented sand: influence of curing time," *Journal of Materials in Civil Engineering*, vol. 23, no. 5, pp. 692–696, 2011.

[19] C. Liu and R. D. Starcher, "Effects of curing conditions on unconfined compressive strength of cement- and cement-fiber-improved soft soils," *Journal of Materials in Civil Engineering*, vol. 25, no. 8, pp. 1134–1141, 2013.

[20] A. Estabragh, M. Khatibi, and A. Javadi, "Effect of cement on the treatment of a clay soil contaminated with glycerol," *Journal of Materials in Civil Engineering*, vol. 28, no. 4, p. 04015157, 2016.

[21] J. Hong, K. Wang, Z. Xiong et al., "Investigation into the freeze-thaw durability of semi-flexible pavement mixtures," *Road Materials and Pavement Design*, vol. 21, no. 1, pp. 1–17, 2019.

[22] H. Yang, L. Jiang, Y. Zhang, and Q. Pu, "Flexural strength of cement paste beam under chemical degradation: experiments and simplified modeling," *Journal of Materials in Civil Engineering*, vol. 25, no. 5, pp. 555–562, 2013.

[23] Research Institute of Highway ministry of Transport, *Test Method of Cement and Concrete for Highway Engineering*, Research Institute of Highway ministry of Transport, Beijing, China, 2005.

[24] American Association of State Highway and Transportation Officials, *Standard Method of Test for Determining the Fracture Potential of Asphalt Mixtures Using Semicircular Bend Geometry (SCB) at Intermediate Temperature*, American Association of State Highway and Transportation Officials, Beijing, China, 2016.

[25] J. Jiang, F. Ni, Q. Dong, F. Wu, and Y. Dai, "Research on the fatigue equation of asphalt mixtures based on actual stress ratio using semi-circular bending test," *Construction and Building Materials*, vol. 158, pp. 996–1002, 2018.